



International Congress of Science and Technology of Metallurgy and Materials, SAM - CONAMET 2013

Corrosion Behaviour of a SiO_xN_y Coated and Nitrided PH Stainless Steel

Eugenia L. Dalibon^{a,b,*}, Mauro Moscatelli^a, Silvia Simison^c, Lisandro Escalada^c, Amado Cabo^d, Carlos Lasorsa^e and Sonia P. Brühl^a

^aSurface Engineering Group, Facultad Regional Concepción del Uruguay, Universidad Tecnológica Nacional, Ingeniero Pereira 676, 3260 Concepción del Uruguay, Argentina.

^bInstituto Sabato (UNSAM – CNEA), Av. Gral. Paz 1499, 1650 Buenos Aires, Argentina.

^cINTEMA, CONICET- Universidad Nacional de Mar del Plata, Juan B. Justo 4302, 7600 Mar del Plata, Argentina.

^dIONAR S.A. Arias 3422, 1430 Buenos Aires, Argentina.

^ePlasma Processing Laboratory, Facultad Regional Haedo, Universidad Tecnológica Nacional. París 532, 1706 Haedo, Argentina.

Abstract

Precipitation hardening stainless steels are used in applications where wear and corrosion resistance are required. To improve the surface properties, thermochemical treatments in combination with hard coatings can be used.

In this work, the corrosion behaviour of SiO_xN_y coatings deposited on nitrided and non-nitrided Corrax® PH stainless steel were evaluated comparing them with the behaviour of samples which were only nitrided (two different conditions of nitrogen percentage in the working gases were used).

The microstructure was analyzed. Corrosion behaviour was evaluated by the Salt Spray Fog Test and cyclic potentiodynamic polarization in NaCl solution. Erosion-corrosion tests were conducted.

The thickness of the coating was about 1.4 microns, and its hardness was 2300 HV. The film had better erosion and corrosion behaviour when it was deposited on the nitrided steel. This fact demonstrated that the nitrided layer results in a good interface that improves the adhesion and mechanical support.

© 2015 The Authors. Published by Elsevier Ltd. This is an open access article under the CC BY-NC-ND license (<http://creativecommons.org/licenses/by-nc-nd/4.0/>).

Selection and peer-review under responsibility of the scientific committee of SAM - CONAMET 2013

Keywords: PH steels, PACVD, Corrosion, plasma nitriding.

1. Introduction

Precipitation hardening stainless steels are used in injection molds for corrosive plastics, medical and food industries and engineering parts where good mechanical properties and corrosion resistance are required. Different

surface treatments can be used in order to improve the surface properties. Plasma nitriding is a thermochemical process that produces a modified layer which has high hardness and good wear resistance but depending on the process conditions the corrosion resistance could be affected due to chromium nitrides precipitation as it was already reported by Esfandiari et al (2007), Dong et al. (2008) and Li et al. (2008) among others.

Given the need to improve the corrosion resistance, a thin film can be deposited by PACVD technique. This would also mean an increase of the surface hardness and wear resistance of the nitrided layer. The oxides, nitrides, oxynitrides and carbides coatings possess low friction coefficient, high mechanical strength and chemical inertness, according to Faines et al. (1997), Zhou et al. (2010) and Li et al. (2010). There are published results concerning the duplex processes (nitriding plus coating) where good tribological performance of the coating-substrate system, stresses reduction at the interface and improved adhesion have been achieved as reported by Zukerman et al. (2007), Qi et al. (2007), Podgornik et al. (2003), Guruvenket et al. (2009) and Benkahoul et al. (2009).

Regarding the corrosion behaviour of the duplex systems, some researchers have reported that the electrochemical behaviour is related not only to the film but to the entire system. It is possible that the films have pores, defects or pinholes and the corrosive media can penetrate the coating and finally reach the substrate, according to Azzi et al. (2010) and Durst et al. (2008). Although there are some published works about this topic, each coating / substrate combination requires a specific study.

In this work, the corrosion and erosion behaviour of a SiN_xO_y film deposited over non-nitrided and nitrided precipitation hardening stainless steels was investigated, and compared with the same steel which was nitrided in two different conditions but not coated.

2. Experimental

Uddeholm Corrax®, a precipitation hardening (PH) stainless steel, was used as base material in this work. The chemical composition in mass percent of Corrax® PH, according to the supplier is 0.03% C, 12% Cr, 1.4% Mo, 0.3% Mn, 0.3% Si, 9.2% Ni, 1.6% Al and Fe as balance. Samples of 6 mm in height were sliced from a bar of 24 mm in diameter, and they were aged at 530 °C for 2 hours according to the supplier recommendations to increase hardness.

Nitriding was carried out for 10 hours in an industrial facility by means of a DC pulsed discharge at 390 °C temperature using two different gas mixtures: 25 % N_2 + 75 % H_2 (samples named N1) and 20 % N_2 + 80 % H_2 (samples named N2). The SiO_xN_y coatings were deposited using the Plasma Assisted Chemical Vapor Deposition technique (PACVD) sustained by a DC pulsed discharge at 700°C with HMDSO and nitrogen as gas precursors. The coatings were deposited on only aged PH stainless steel (samples named “C”) and on N2 nitrided samples (samples named “D”). Samples of PH stainless steel which were only aged were used as the control group (named P).

The surface hardness in the nitrided samples was assessed with a Vickers micro indenter, with 50 g load. The hardness of the films was measured employing a nanoindenter with Berkovich tip and 10 mN load. The microstructure of the films and the nitrided layers was characterized by optical microscopy (OM) and SEM equipped with Focus Ion Beam (FIB). The nitrided layers were analyzed by X-ray diffraction using $\text{K}\alpha$ Cu radiation.

The corrosion behaviour was evaluated using the Salt Spray Fog Test according to ASTM B117 standard. These tests were conducted in 5% NaCl solution, pH 6.8, at 32 °C, during 100 h. Results were evaluated qualitatively, observing the presence of rust, and quantitatively, after taking a digital photograph. The photographs were analyzed with the software Scion Image® to obtain the percentage of the surface where general corrosion could be observed. Pits were observed and measured with OM and only those with areas larger than 0.01 mm² were reported.

Electrochemical experiments were conducted at room temperature and atmospheric pressure in a three-electrode cell. A saturated calomel electrode (SCE) was employed as the reference electrode and a platinum spiral wire as the counter electrode. Corrosion resistance was evaluated by means of cyclic potentiodynamic polarization using a VoltaLab PGZ 402 potentiostat. The potential was scanned at a sweep rate of 1mV/s between the corrosion potential and the sweep reversal potential, which was arbitrarily chosen to attain a current density of 200 $\mu\text{A}/\text{cm}^2$, as it was published in a previous work, Escalada et al., 2013.

After the corrosion experiments, the surface morphology was examined using OM and SEM and the surface composition in different regions was estimated using EDS. Erosion resistance was tested in a mixture of sea water

and sand (AFS GFN of 50) flux during 20 hours at a temperature of 60 °C. The samples rotated in the slurry solution at a mean tangential velocity of 7 m/s. Before and after the tests the samples were weighed with a ScienTech analytical balance, 0.1 mg readability. Mass loss relative to the mass loss of the only aged PH steel samples was calculated to evaluate the effect of surface modification on erosion resistance. The eroded surfaces were examined by means of OM.

3. Results and discussion

3.1. Hardness and microstructure

The PACVD SiO_xN_y films were deposited on nitrated and non nitrated PH stainless steel and reached a thickness of 1.4–1.5 μm in both cases (Fig.1). These films could be described as amorphous and non-stoichiometric silicon oxynitride, confirmed by FTIR, XRD and EDS (Dalibon et. al, 2011).

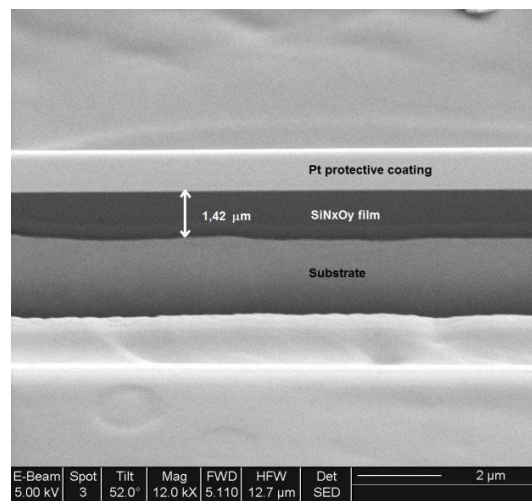


Fig. 1. (a) SEM-FIB view of the film on PH stainless steel (C).

The nitrated layer in both conditions is composed of a white layer and a diffusion zone beneath. The white layer can be observed near the surface (Fig. 2) with a not very well defined interface with the non-affected substrate.

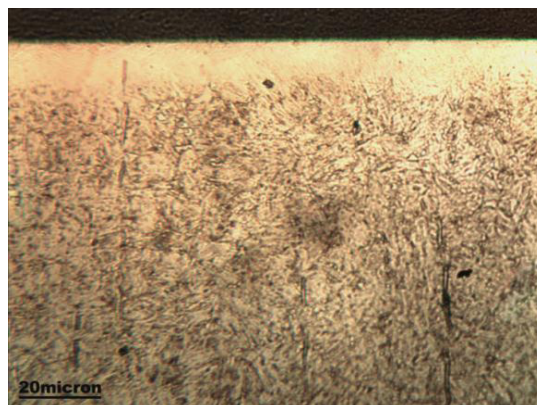


Fig.2. Optical micrograph of N2 sample.

The nitrided layer was thicker in the condition N1 with higher nitrogen content in the gas mixture than in the condition N2 (Table 1).

Table 1. Hardness and thickness of the nitrided layers in N1 and N2 or the coating in D and C.

Samples	Hardness (HV)	Thickness of nitrided layers or the coating (μm)
N1	1420 ± 30	18 ± 1
N2	1240 ± 60	14 ± 1
D	2300 ± 300	1.4–1.5
C	2300 ± 300	1.4–1.5
P	580 ± 50	-

The XRD analysis revealed α'_N peaks that correspond to nitrogen supersaturated martensite or the so called “expanded martensite”. The martensite peaks are shifted to lower angles showing a lattice expansion, and they are also broader, especially in the N1 nitriding condition, indicating that the nitriding process generates microstresses and defects. In addition, γ_N peaks were detected, and they correspond to retained austenite that was converted into expanded austenite after nitriding (Brühl et. al, 2010; Dong et. al, 2008). Chromium nitrides (CrN) peaks were only detected in the sample nitrided in N1 condition with higher nitrogen content in the gas mixture (Fig. 3).

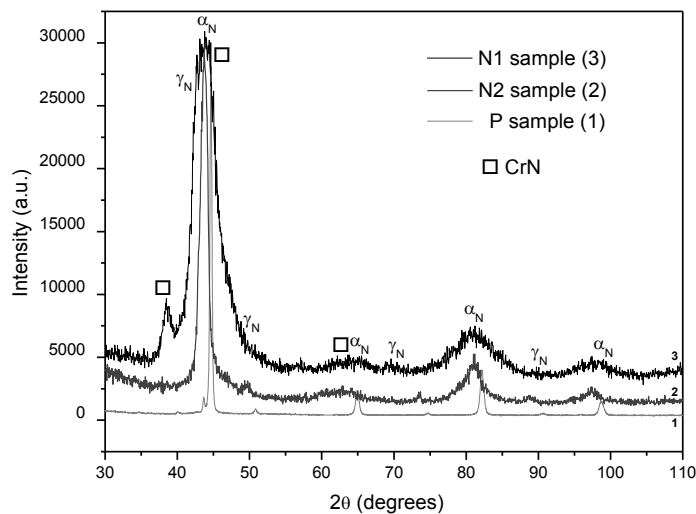


Fig.3. XRD patterns of the nitrided samples superimposed with the ones of the only aged PH steel.

The coating hardness in C and D samples was similar and reached 2300 ± 300 HV (measured with the Berkovich indenter and converted to Vickers). As indentation depth does not exceed 10% of the film thickness the obtained value is not influenced by the substrate properties (Jedrzejowski et al. (2003)). The nitrided layer hardness was higher in the N1 sample with major nitrogen content in the gas mixture than in the N2 sample (Table 1).

3.2. Corrosion behaviour

After 100 hours exposure in the salt spray fog test, the PH steel, N2, D and C samples were clean with no sign of general or localized corrosion. On the other hand, the N1 sample presented a region of general corrosion,

approximately 47% of the exposed area (Fig. 4) and a large number of pits, but only three of them with an area greater than 0.01 mm^2 .

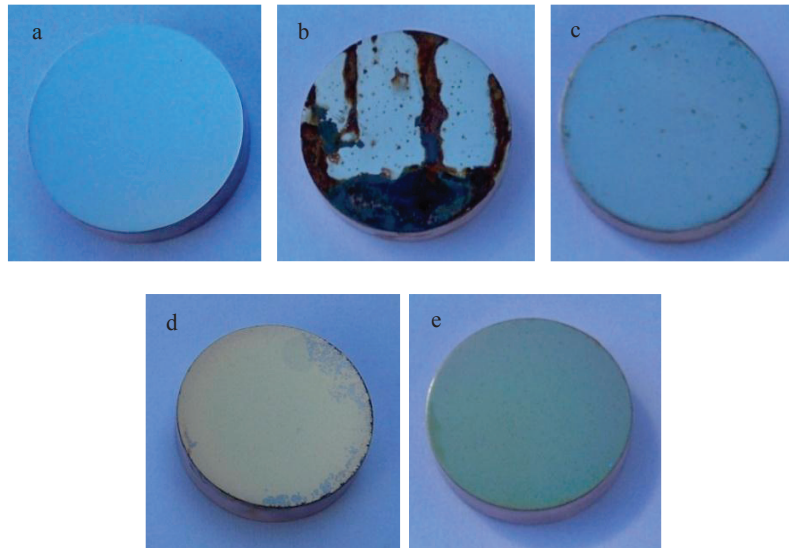


Fig. 4. Surface aspect of the different samples after salt spray fog test a) P, b) N1, c) N2, d) D, e) C

In the electrochemical tests of the nitrided samples and the only aged PH steel, the N2 nitrided layer had nobler breakdown potential than the other samples as it can be seen in the polarization curves (Fig.5). The N1 sample presented almost no passive region but only active dissolution. This is in agreement with previous observations (Li et. al (2004), Brühl et. al. (2010) and Escalada et al (2013)) that indicate that nitrogen has a beneficial effect when it is in solid solution. If chromium nitrides (CrN) precipitates are formed, the chromium content in the matrix is reduced, and the corrosion resistance decreases.

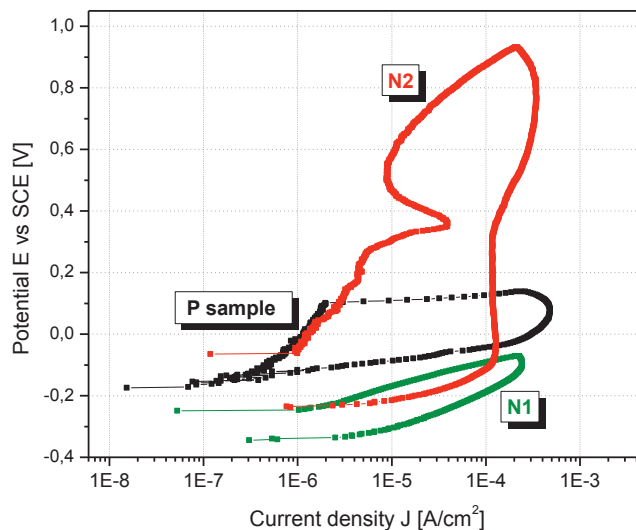


Fig. 5. Cyclic polarization curves of nitrided samples and aged PH sample.

Regarding the corrosion resistance of the only coated samples (C), they presented a small passive region and its breakdown potential does not differ much from that of the aged PH sample (Fig. 6). This behaviour may be related to the presence of adhesion defects in the film-substrate interface which could result in initiation sites for crevice corrosion.

The D sample presented an improvement on the localized corrosion resistance. The breakdown potential was nobler than those corresponding to the other samples as it can be observed in the cyclic polarization curves (Fig. 6), it reached 1 V above the corrosion potential. This value has been already registered by other researchers for silicon nitride coatings such as Li et al (2010).

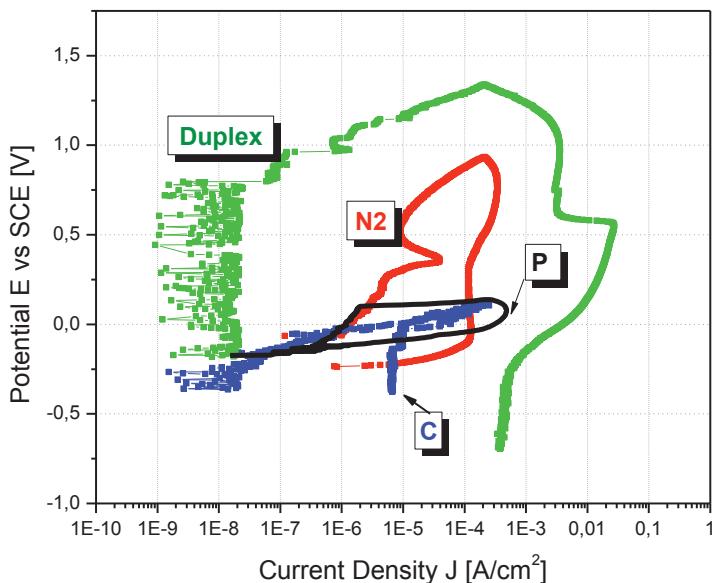


Fig. 6. Cyclic polarization curves of C, D, N2 and P samples.

In figure 7a, a pit can be observed and the film is about to break off and detach, it is proposed that the current response in Figure 6 is due to corrosion initiation in a small defect where a pit is formed. When the steel is corroded under the coating, the mechanical support of the film is affected, and then it collapses exposing a larger area of the steel surface as it can be observed in figure 7b, producing a large increase in the current density with the accumulation of non-very protecting corrosion products in the pit entrance or under the film, the current resulted controlled by mass transfer in the reverse sweep.

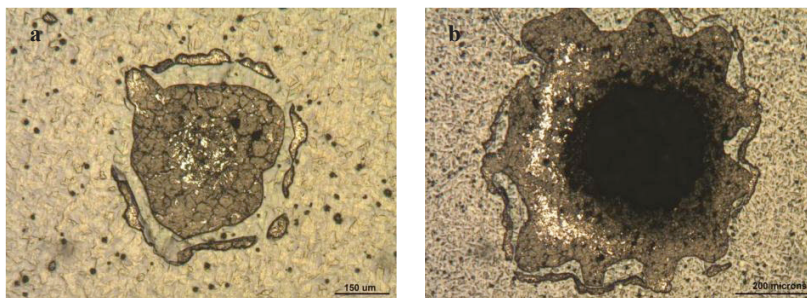
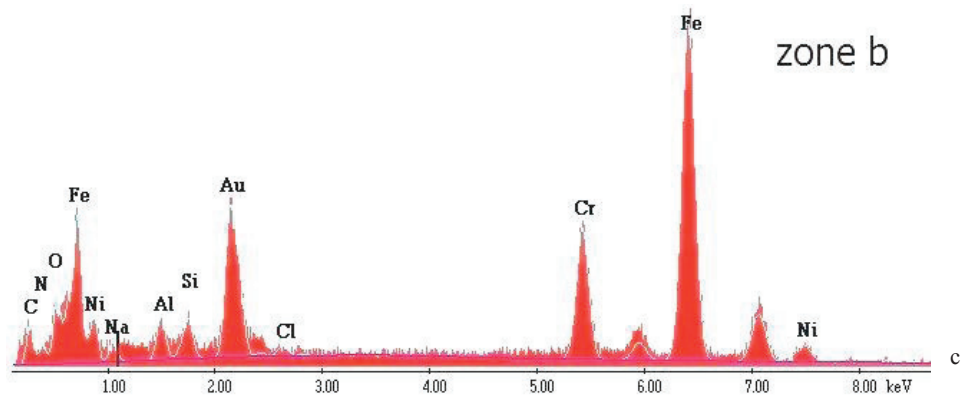
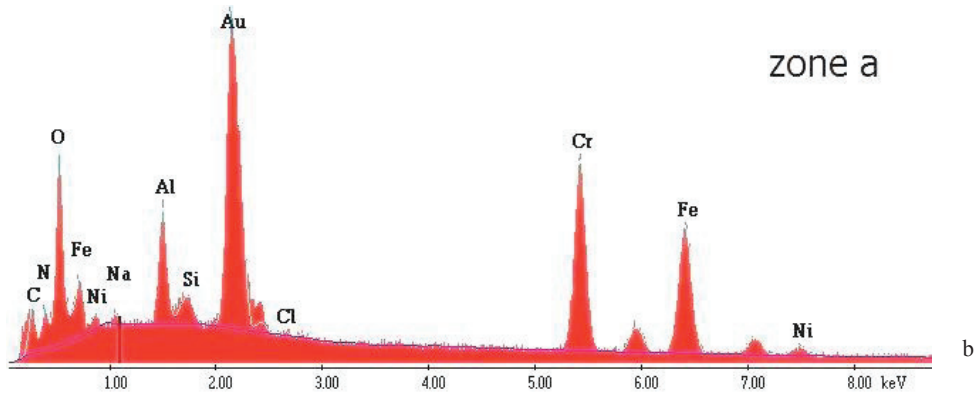
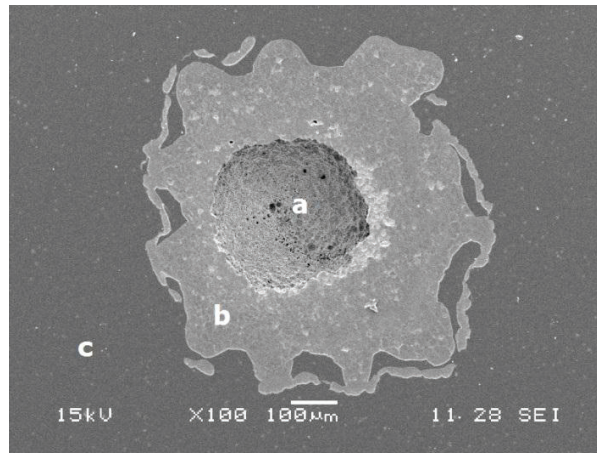


Fig. 7. Optical micrograph of two pits in the duplex sample (D).

The corroded region was analyzed by means of SEM and EDS (Fig. 8). It could be observed that in the clearer zones, the coating was detached because the silicon signal was not detected (Fig.8a and b) and the darker zones are still covered with the coating (Fig. 8c). In addition, in the SEM image some detachment of the film around the pit can be observed, indicating that adhesion was not very good.



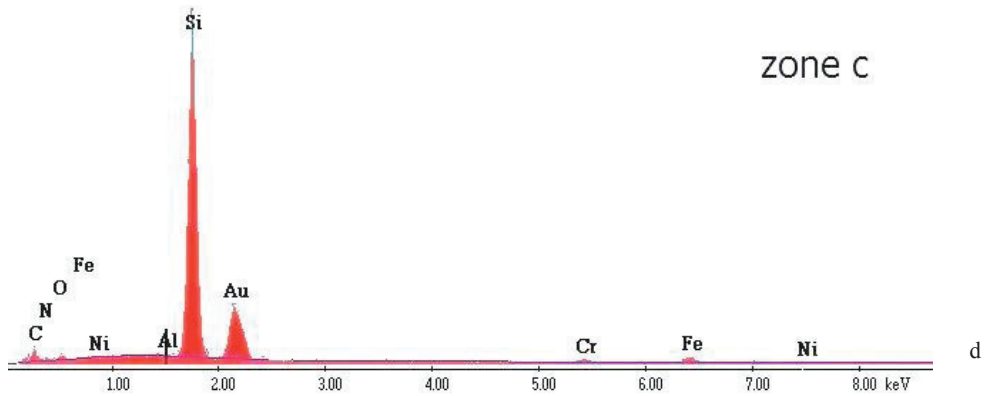


Fig. 8. a) Corrosion pit in sample D, b), c) and d) EDS of different regions of the corroded surface.

3.3. Erosion behaviour

The erosion behaviour in the D and N2 samples was similar; the mass loss was about 50 % of that in the P sample (Fig. 9). The nitrated layer plus the hard coating can be a good combination to resist the erosion test. It is possible that this behavior is related not only to the hardness but also to the fracture toughness and resistance to plastic deformation of the nitrated layer and of the coating as it was pointed out by Zukerman et al. (2007) and Bousser et al (2008).

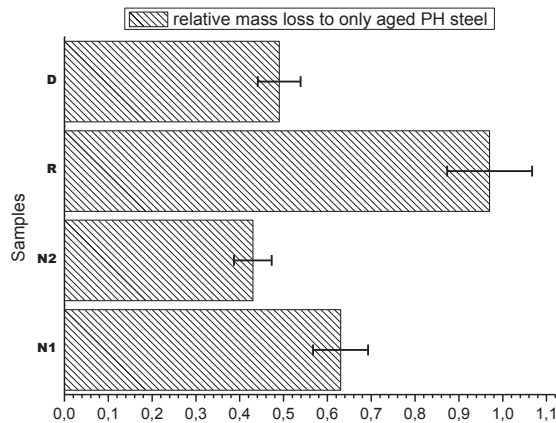


Fig. 9. Erosion results: relative mass loss to only aged PH steel.

The erosion behaviour of the coated sample was similar to the only aged PH steel since the mass loss was 3% lower than in the P sample (Fig. 9) It is possible that the coating was detached a few minutes after the test started, and the impact of erosive particles was produced on PH steel substrate.

Regarding the eroded surface, no noticeable differences were observed between N2 and D samples, only in the C sample a severe damage was observed as it is shown in figure10.

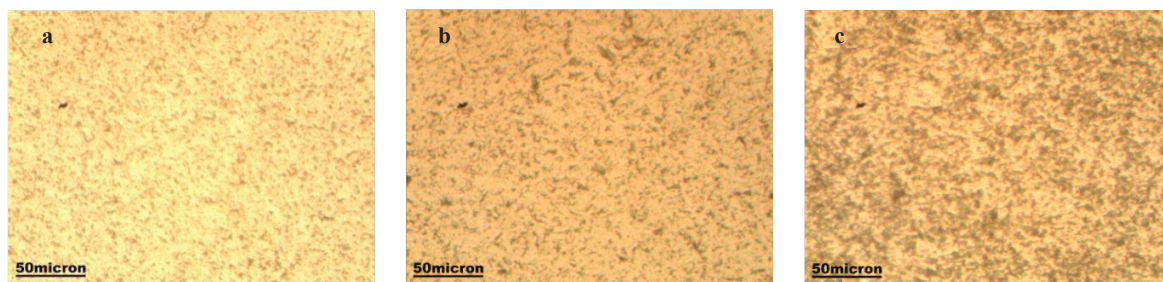


Fig. 10. Optical micrographs of eroded surfaces: a) N2, b) D, c) C.

4. Conclusions

Amorphous SiOxNy thin films over PH stainless steels are erosion resistant only if deposited on a previous nitrided layer which improved the substrate hardness, the resistance to plastic deformation and to the erosion caused by the impact of hard particles.

Moreover, both erosion and corrosion tests showed that the film deposited on the nitrided layer with 20% nitrogen seemed to have a good interface and a better adhesion than the one on the non nitrided PH steel. It would be not recommendable to deposit this kind of film over non nitrided steel if erosion resistance is needed, since the coating was broken by the impact of hard particles because the substrate was not hard enough to provide load bearing capacity.

The mechanism of film breakdown needs to be further studied in order to determine if the increase in current density in the polarization curves is due to pre-existing flaws or to electrical disruption. Future work will be directed to characterize the corrosion resistance of the coating as a function of both the substrate and the interface.

Acknowledgements

The authors would like to thank to Dr. M. Agustina Guitar and the Saarland University (Germany) for the SEM-FIB analysis and to Dr. Mariela Desimone (INTEMA) for XRD measurements.

References

- Azzi, M., Benkahoul, M., Klemberg-Sapieha, J. E., Martinu, L., 2010. Corrosion and mechanical properties of duplex-treated 301 stainless steel. *Surface and Coatings Technology* 205, 1557-1563.
- Benkahoul, M., Robin, P., Martinu, L., Klemberg-Sapieha, J. E., 2009. Tribological properties of duplex Cr-Si-N coatings on SS410 steel. *Surface and Coatings Technology* 203, 934-940.
- Bousser, E., Benkahoul, M., Martinu, L., Klemberg-Sapieha, J. E., 2008. Effect microstructure on erosion resistance of Cr-Si-N coatings. *Surface and Coatings Technology* 203, 776-780.
- Brühl, S. P., Charadia, R., Simison, S., Lamas, D. G., Cabo, A., 2010. Corrosion behavior of martensitic and precipitation hardening stainless steels treated by plasma nitriding. *Surface and Coatings Technology*. 204, 3280-3286.
- Dalibon, E. L., Lasorsa, C., Cabo, A., Cimetta, J., García, N., Brühl, S. P., 2012. Tribological properties of SiNx films on PH stainless steel with and without nitriding as a pre-treatment. *Procedia Materials Science* 1, 313-320.
- Dong, H., Esfandiari, M., Li, X. Y., 2008. On the microstructure and phase identification of plasma nitrided 17-4PH precipitation hardening stainless steel. *Surface and Coatings Technology* 202, 2969-2975.
- Durst, O., Ellermeier, J., Berger, C., 2008. Influence of plasma nitriding and surface roughness on the wear and corrosion resistance of thin films (PVD/PECVD). *Surface and Coatings Technology* 203, 848-854.
- Escalada, L., Lutz, J., Brühl, S. P., Fazio M., Márquez, A., Mandl, S., Manova, D., Simison, S. N., 2013. Microstructure and corrosion behaviour of AISI 316L duplex treated by means of ion nitriding and plasma based ion implantation and deposition. *Surface and Coatings Technology* 223, 41-46.
- Esfandiari, M., Dong, H., 2007. The corrosion and corrosion-wear behaviour of plasma nitrided 17-4PH precipitation hardening stainless steel. *Surface and Coatings Technology* 202, 466-478.
- Fainer, N. I., Rumyantsev, Y. M., Kosinova, M. L., Yurjev, G. S., Maximovskii, E. A., Kuznetsov, F. A., 1997. The investigation of properties of silicon nitride films obtained by PECVD from hexamethyldisilazane. *Applied Surface Science* 113-114, 614-617.
- Guruvenket, S., Li, D., Klemberg-Sapieha, J. E., Martinu, L., Szpunar, J., 2009. Mechanical and tribological properties of duplex treated TiN, nc-TiN/a-SiNx and nc-TiCN/a-SiCN coatings deposited on 410 low alloy stainless steel. *Surface and Coatings Technology* 203, 2905-2911.

- Jedrzejski, P., Klemberg-Sapieha, J. E., Martinu, L., 2003. Relationship between the mechanical properties and the microstructure of nanocomposite TiN/SiN_{1.3} coatings prepared by low temperature plasma enhanced chemical vapor deposition. *Thin Solid Films* 426, 150-159.
- Li, C. X., Bell, T., 2004. Corrosion properties of active screen plasma nitrided 316 austenitic stainless steel. *Corrosion Science* 46, 1527–1547
- Li, D., Gurusanket, S., Azzì, M., Szpunar, J. A., Klemberg-Sapieha, J. E., Martinu, L., 2010. Corrosion and tribo-corrosion behavior of a-SiC_x:H, a-SiN_x:H and a-SiC_xN_y:H coatings on SS301 substrate. *Surface and Coatings Technology* 204, 1616–1622.
- Li, G.-J., Wang, J., Li, C., Peng, Q., Gao, J., Shen, B.-L., 2008. Microstructure and dry-sliding wear properties of DC plasma nitrided 17-4 PH stainless steel. *Nuclear Instruments and Methods in Physics Research Section B* 266, 1964-1970.
- Podgornik, B., Vižintin, J., 2003. Tribology of thin films and their use in the field of machine elements. *Vacuum* 68, 39–47.
- Qi, F., Leng, Y. X., Huang, N., Bai, B., Zhang, P. Ch., 2007. Surface modification of 17-4PH stainless steel by DC plasma nitriding and titanium nitride film duplex treatment. *Nuclear Instruments and Methods in Physics Research B* . 257, 416–419.
- Zhou, F., Yu, B., Wang, X., Wu, X., Zhuge, L., 2010. Surface roughness, mechanical properties and bonding structure of silicon carbon nitride films grown by dual ion beam sputtering. *Journal of Alloys and Compounds* 492, 269–276.
- Zukerman, I., Raveh, A., Landau, Y., Weiss, R., Shneck, R., Shneor, Y., Kalman, H., Klemberg-Sapieha, J. E., Martinu, L., 2007. Tribological properties of duplex treated TiN/TiCN coatings on plasma nitrided PH15-5 steel, *Surface and Coatings Technology* 201, 6171-6175.